

The formation and dynamics of sediment waves

G.M. Keevil & J. Peakall

Earth and Biosphere Institute, School of Earth and Environment, University of Leeds, Leeds, LS2 9JT. UK

J.L. Best

Departments of Geology and Geography, University of Illinois at Urbana-Champaign, Urbana, Illinois 61801, USA

ABSTRACT: Overspill from submarine channels is known to be responsible for the formation and maintenance of sediment waves on backside levee slopes. The morphology of these sediment waves is controlled by the distribution of channel overspill. There are currently no published measurements of channel overspill, so little is known about the velocity or concentration structure.

This paper presents the results from a series of experiments in which saline gravity currents flowed over an erodible sediment bed in the base of a fixed form submarine channel model. This resulted in the deposition of overbank sediment waves associated with channel overspill at the apex of channel bends. Ultrasonic Doppler velocity profiling was used to quantify the flow field responsible for the deposition of the sediment waves.

The results from this study provide detailed insights into the process of sediment wave initiation and also provide quantified evidence for the structure of the flow field responsible for the deposition of the sediment waves. The sediment waves were deposited in the lee of a hydraulic jump, where the hydraulic jump was formed as the fluid overspilling the channel model decelerated at the break in slope at the base of the overbank slope. The results of this study suggest that the presence of sediment waves on channel levees are intrinsic to the process of channel overspill, where the backside levee slope is sufficiently large to induce a hydraulic jump or where a single flow is large enough to initiate a hydraulic jump within the overspill flow.

1 INTRODUCTION

Sediment waves are common features on submarine channel levees (McHugh & Ryan, 2000; Normark et al., 2002b; Wynn & Stow, 2002) and are especially common within topographically constrained channel systems such as the Hikurangi Trough, Joshua Channel and the Toyama channel (Lewis, 1994; Nakajima et al., 1998; Lewis & Pantin, 2002; Posamentier, 2003; Posamentier & Kolla, 2003). Such sediment waves have a typical wavelength of 300-6000 m and a height of 3-20 m. The crests are typically orientated oblique to the channel axis (Migeon et al., 2000; Normark et al., 2002b) and due to the effect of the Coriolis force they are typically found on the right-hand levees of submarine channel systems (left-hand in the southern hemisphere) (Normark et al., 2002a).

Seismic studies of sediment waves have shown they have a very characteristic internal morphology (Nakajima et al., 1998; Ercilla et al., 2002a; Lewis & Pantin, 2002; Normark et al., 2002a), with the upslope flanks being thicker than the downslope flanks and containing coarser sediment (Ercilla et al.,

2002a). The observed sediment wave asymmetry leads to considerable lateral migration, with rates as high as 20 m/1000 yr (Lewis & Pantin, 2002). There are two general models for the formation of sediment waves, the first model suggests that antidune flow conditions are responsible, through the generation of internal waves which govern the sediment wave morphology (Normark et al., 1980; Wynn et al., 2000a; Ercilla et al., 2002a; Ercilla et al., 2002b), the second model suggests that sediment waves are generated by the action of internal lee waves (Lewis & Pantin, 2002). The antidune model is often invoked to explain the upslope migration, but requires a Froude number close to unity, which in turn imposes strict hydrodynamic conditions to comply with this. The lee wave model requires less strict hydrodynamic conditions, but cannot be readily used to explain the upslope motion of sediment waves. However, other factors such as the action of hemipelagic deposition and turbidity current frequency/intensity have also been shown to be important in the formation of sediment waves (Wynn et al., 2000b; Wynn & Stow, 2002). Wynn & Stow (2002) suggest that the process of sediment wave

migration and growth is self-perpetuating after the initial wave topography is established. Both numerical and experimental modelling have shown that sediment waves can continue to develop and migrate under subcritical flow conditions, where the existing topography acts to capture more sediment on the up-slope flanks through the processes of flow deceleration and topographic blocking (Kubo & Nakajima, 2002; Lee et al., 2002). The processes that control sediment wave initiation are still largely unknown; the existing models of sediment wave formation are based on seismic, bathymetric and some basic hydrodynamic interpretation. However, neither of these two existing models fully explains the process of sediment wave initiation and formation.

2 METHODOLOGY

The experiments described in this paper concern extra-channel sedimentation and the formation of bedforms associated with overspill from a sinuous submarine channel model. The experiments were conducted within a square flume tank (1.8 m by 1.8 m, depth 1.7 m), saline fluid entered the flume tank via a 2 m long input channel centred on one of the faces of the square channel (Fig. 1). The saline fluid was allowed to flow through a preformed glass-reinforced plastic model. The channel model has a planform which consists of a series of arcs of constant radius separated by straight sections, giving a sinuosity of 1.36 (Fig. 1).

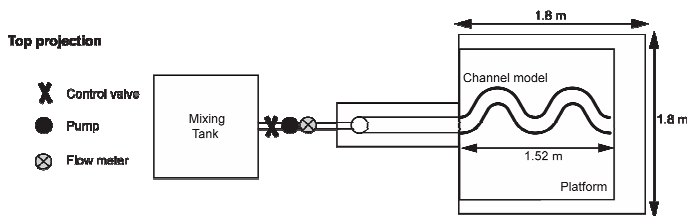


Figure 1. Schematic planform view of flume facility illustrating the mixing tank and the position of the channel model

Flow velocities were recorded on the channel overbank area using Ultrasonic Doppler Velocity Profiling (UDVP). UDVP measures velocity by emitting a beam of ultrasound and then recording the frequency of sound reflected by particles suspended in the flow, the Doppler shift is then calculated between the emitted and recorded frequency (Takeda 1991, 1993, Best et al., 2001). These experiments utilised ten 4 MHz UDVP transducers, each of which was configured to calculate a profile consisting of 128 velocity measurements equally spaced along the axis of the ultrasound emission. Each profile was separated by a delay of 15 ms, the measurement time was 7-11 ms, and thus the overall measurement time was near instantaneous.

Scale modelling of submarine channels is not possible as there is currently no data set available from which a comprehensive prototype could be constructed, therefore, these experiments adopted an analogue modelling approach, the aim of which is to successfully create 'similarity of process' with a natural system (Hooke, 1968). Analogue models are not scaled from a specific prototype or ratio of forces, but aim to reproduce genetic processes and features observed within a natural system. Analogue modelling has been used extensively to model fluvial systems, greatly improving our understanding of process product relationships (Leopold and Wolman, 1957; Schumm and Khan, 1972; Schumm et al., 1987). Analogue modelling has also previously been used to study submarine channel processes (Métivier et al., 2005; Keevil et al., 2006; Peakall et al., 2007).

3 EXPERIMENTAL RESULTS

Four successive density currents (density 1025 kg m^{-3}) were released through the channel model (Fig. 1) over an erodible bed of low density plastic polymer sediment (25 -35 mm thick). Each successive density current was released over the bathymetry formed by the previous experiment, and the bathymetry was recorded (Fig. 2, only the final bathymetry is shown). The duration of the four currents was not constant, but chosen to record the development of intra-channel bedforms (Amos et al. 2004a,b), the duration of each experiment is shown in Fig. 3. During these experiments the only sediment supply came from the initial deposit within the channel model, so all the material comprising the overbank bedforms was reworked from within the channel model, by the action of the dense saline fluid.

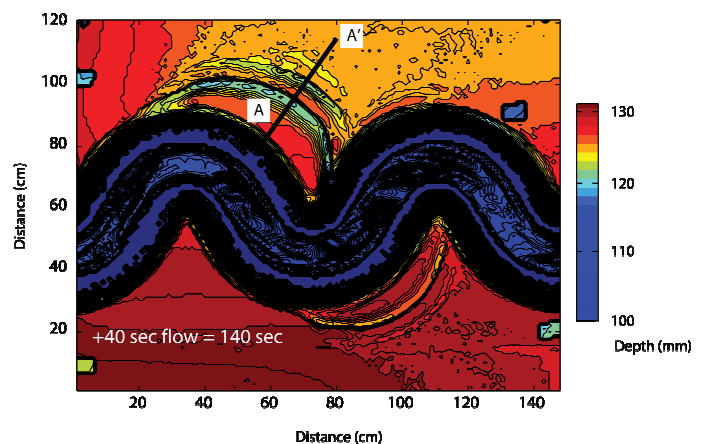


Figure 2. Temporal development of overbank bedforms, illustrating the position of the transect A-A', final surface after 140 seconds of flow.

The four successive experiments resulted in the deposition of a series of lunate bedforms situated overbank from the apexes of the first and second bends (Fig. 2). These bedforms started to develop

within 60 seconds of the passage of the density current head through the channel model. The bedforms

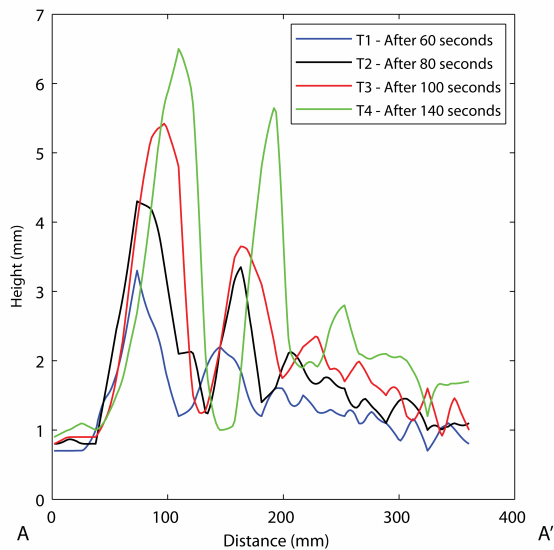


Figure 3. Temporal development of overbank bedforms along the transect A-A', the location of the profile is shown in Fig. 2. The final temporal profile is illustrated in Fig. 2.

at the apex of the first bend developed faster and were higher than those beyond the apex of the second bend. The transect A-A' illustrates the temporal development of the overbank bedforms (Fig. 3, located on Fig. 2), the bedforms developed three distinct crests, decreasing in height distally from the axis of the channel. The transects illustrate that the bedforms crests grew in height and migrated away from the channel axis as a function of time. In contrast, the bedform wavelength remained constant through time.

To investigate the velocity distribution of the flow responsible for the deposition of the overbank bedforms, a second series of experiments was carried out using the same experimental model with a mobile sediment bed and the same discharge and saline density (1025 cm³ s⁻¹ and 1025 kg m³, respectively). During this second series of experiments an array of 10 UDVP transducers was positioned to record the velocity along the transect A'-A (orientated at the edge of the overbank region facing towards the apex of the first bend of the channel model (Fig. 3)). The initial plot of velocity distribution (Fig. 4A), shows the time-averaged velocity distribution (30 seconds of data recorded after the passage of the head through the channel model) over the initial flat experimental surface. The second plot of velocity distribution (Fig. 4B), shows the time-averaged velocity distribution (using the same relative temporal window) over the final experimental surface after 840 seconds of flow has passed over the surface, the developed bedforms are illustrated at the base of the figure. Both of the plots of velocity show the same overall velocity distribution (Figs. 4A and 4B). The

highest velocity was found at the extreme right of the plots approximately 450 mm from the origin, this is related to fluid plunging over the levee crests of the channel model; the outside levee crest is positioned 520 mm from A'. Another extensive region of high velocity was found proximal to the origin of the transect on the flat experimental surface (Fig. 4A). After the development of the bedforms, the second region of high velocity has significantly altered when compared with the results recorded over the initial experimental surface. The regions of highest velocity are found between the bedform crests and the entire region of high velocity has migrated ~100 mm towards the channel model.

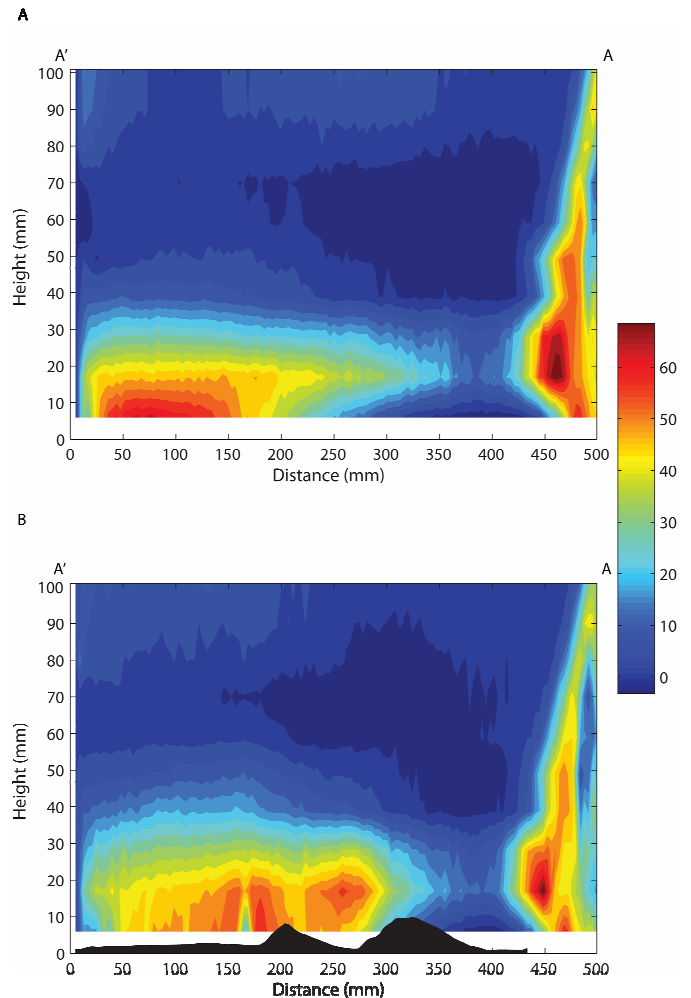


Figure 4. Time-averaged (30 seconds) velocity distribution along the transect A'-A. A. Velocity distribution along the transect A'-A across the initial flat perturbation free experimental surface prior to the formation of any bedforms. B. Velocity distribution along the transect A'-A after 840 seconds of flow.

4 DISCUSSION

When an erodible sediment bed was deposited within the channel model, it aided visualisation of overspill processes, this visualisation came from the deposition of a number of flow transverse bedforms on the flat outer channel margin beyond the levee backslope. The position and general morphology of

these bedforms suggest that they may be analogous to sediment waves which are common within natural submarine channel levee systems (McHugh & Ryan, 2000; Normark et al., 2002A; Fildani et al. 2006). The overbank bedforms consist of a series of lunate crests which are positioned downslope from the apex of the first and second bends of the channel model.

Along the transect A-A' just beyond the break of slope on the flat experimental surface, the overspill velocity is seen to drop and then increase with increasing distance from the channel model (Fig. 4A). Detailed time-averaged measurements along the transect A'-A, at or just above the break of slope between the channel model and experimental surface, reveal the presence of an accelerating region of fluid. Time-averaged estimates of the thickness of this fluid (h_o) vary between 10-20 mm and estimates of the Froude number for the overbank flow on the levee backslope are 0.5-1.8; the variability of h_o is reflected within the estimate of the Froude number

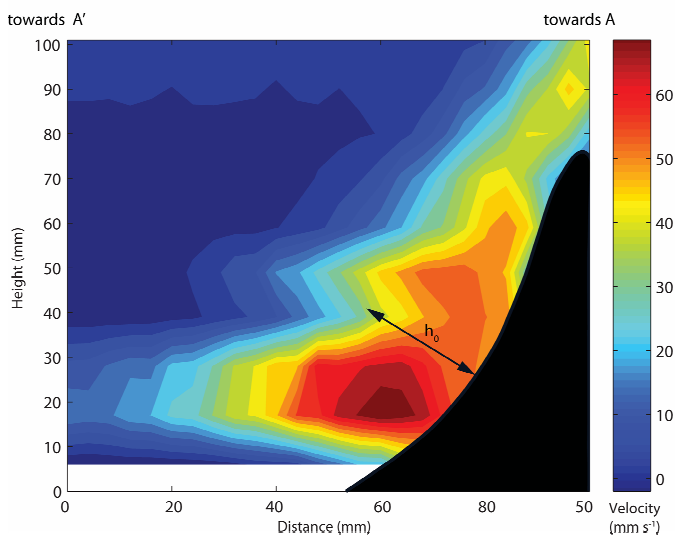


(Fig. 5).

Figure 5. Detailed time-averaged (30 second mean) velocity distribution measured at the break of slope between the channel model and experimental surface along the transect A'-A. The position of the transect is oblique to the orientation of the channel axis normal to the centre of the sediment waves. The positive velocity is flowing away from the axis of the channel model and negative velocity is flowing towards the axis of the channel model. The position of the outer channel levee is highlighted by the black mask.

Detailed analysis of the Froude number along the transect A'-A reveals the presence of a hydraulic jump at the base of the backside levee slope. The crest of the proximal bedform is positioned just downstream of the hydraulic jump and the entire bedform is in the lee of this hydraulic jump. The location of the observed overbank bedforms is a function of the overbank velocity distribution and the successive bedform crests are separated by perturbations in the velocity distribution (Fig. 4B). These perturbations may be due to internal waves resulting from the combined effects of the break of slope be-

tween the channel model and experimental surface, and the hydraulic jump at this break of slope. The deceleration of the overbank flow at the hydraulic jump results in instantaneous deposition of suspended sediment and will also act to reduce the imposed shear stress resulting in a reduction in the rate of tractional transport immediately downstream of the hydraulic jump (García and Parker, 1993).

5 CONCLUSIONS

The results of this study suggest that the presence of sediment waves on channel levees are intrinsic to the process of channel overspill, where the backside levee slope is sufficiently large to induce a hydraulic jump or where a single flow is large enough to initiate a hydraulic jump within the overspill flow. The presence of a hydraulic jump would induce sedimentation and initiate sediment waves. The same flow conditions would not be required subsequently for the aggradation and migration of sediment waves, as the presence of the initial topography would be enough to ensure further development (Kubo & Nakajima, 2002; Lee et al., 2002). This paper for the first time provides a mechanism for the initiation of sediment waves that is also able to explain the observed spatial variations in sediment wave distribution and morphology.

6 REFERENCES

- Amos, K., Peakall, J., Gupta, S., Keevil, G. M., and Laursen, Y. (2004a). The topography of sediment reworked by gravity current flow in sinuous submarine channels. *BSRG Annual Meeting, Manchester* (Abstract).
- Amos, K., Peakall, J., Gupta, S., and Laursen, Y. (2004b). Experimental models of gravity current flow in sinuous submarine channels: flow structure and deposit characteristics. *NERC Ocean Margins LINK Meeting, London* (Abstract).
- Ercilla, G., Alonso, B., Wynn, R. B., and Baraza, J. (2002a). Turbidity current sediment waves on irregular slopes: observations from the Orinoco sediment-wave field. *Marine Geology* 192, 171-187
- Ercilla, G., Wynn, R. B., Alonso, B., and Baraza, J. (2002b). Initiation and evolution of turbidity current sediment waves in the Magdalena Turbidite System. *Marine Geology* 192, 153-169
- Fildani, A., Normark, W.R., Kostic, S. and Parker, G. (2006) Channel formation by flow stripping: large scale scour features along the Monterey East Channel and the relation to sediment waves. *Sedimentology* 53, 1-23
- García, M. and Parker, G. (1993). Experiments on the entrainment of sediment into suspension by a dense bottom current. *Journal of Geophysical Research* 98, 4793-4807
- Hooke, R. (1968). Model Geology: prototype and laboratory stream: Discussion. *Geological Society of America Bulletin* 79, 391-393
- Keevil, G.M., Peakall, J., Best, J.L., Amos, K.J., 2006. Flow structure in sinuous submarine channels: velocity and turbulence structure of an experimental submarine channel. *Marine Geology* 229, 241-257.

- Kubo, Y. and Nakajima, T. (2002). Laboratory experiments and numerical simulation of sediment- wave formation by turbidity currents. *Marine Geology* 192, 105-121
- Lee, H. J., Syvitski, J. P. M., Parker, G., Orange, D., Locat, J., Hutton, E. W. H., and Imran, J. (2002). Distinguishing sediment waves from slope failure deposits: field examples, including the 'Humboldt slide' and modelling results. *Marine Geology* 192, 79-104
- Leopold, L.B., Wolman, M.G., 1957. River channel patterns: braided, meandering and straight. *US Geological Survey, Professional Paper* 282B, pp. 39–85.
- Lewis, K. B. (1994). The 1,500 km long Hikurangi Channel: an axial channel that escapes its trench, crosses a plateau and feeds a fan-drift. *Geo-Marine Letters* 14, 19-28
- Lewis, K. B. and Pantin, H. M. (2002). Channel-axis, overbank and drift sediment waves in the southern Hikurangi Trough, New Zealand. *Marine Geology* 192, 123-151
- McHugh, C. M. G. and Ryan, W. B. F. (2000). Sedimentary features associated with channel overbank flow: examples from the Monterey Fan. *Marine Geology* 163, 199-215
- Metivier, F., Lajeunesse, E., and Cacas, M. C. (2005). Submarine canyons in the bathtub. *Journal of Sedimentary Research* 75, 6-11
- Migeon, S., Savoye, B., and Faugetes, J.-C. (2000). Quaternary development of migrating sediment waves in the Var deep-sea fan: distribution, growth pattern and implication for levee evolution. *Sedimentary Geology* 133, 265-293
- Nakajima, T., Satoh, M., and Okamura, Y. (1998). Channel-levee complexes, terminal deep-sea fan and sediment wave fields associated with the Toyama Deep-Sea Channel system in the Japan Sea. *Marine Geology* 147, 24-41
- Normark, W. R., Hess, G. R., Stow, D. A. V., and Bowen, A. J. (1980). Sediment waves on the Monterey fan levee: A preliminary physical interpretation. *Marine Geology* 37, 1-18
- Normark, W. R., Piper, D. J. W., Posamentier, H., Pirmez, C., and Migeon, S. (2002a). Variability in form and growth of sediment waves on turbidite channel levees. *Marine Geology* 192, 23-58
- Normark, W. R., Piper, D. J. W., Posamentier, H., Pirmez, C., and Migeon, S. (2002b). Variability on form and growth of sediment waves on turbidite channel levees. *Marine Geology* 192, 23-58
- Peakall, J., Amos, K.J., Keevil, G.M. Bradbury, P. and Sanjeev, G. (2007) Flow processes and sedimentation in submarine channel bends. *Marine and Petroleum Geology* 24, 470-486.
- Posamentier, H. W. (2003). Depositional elements associated with a basin floor channel-levee system: case study from the Gulf of Mexico. *Marine and Petroleum Geology* 20, 667-690
- Posamentier, H. W. and Kolla, V. (2003). Seismic geomorphology and stratigraphy of depositional elements in deep-water settings. *Journal of Sedimentary Research* 73, 367-388
- Schumm, S. A. and Khan, H. R. (1972). Experimental study of channel patterns. *Geological Society of America Bulletin* 88, 1755-1770
- Schumm, S. A., Mosley, M. P., and Weaver, W. E. (1987). *Experimental Fluvial Geomorphology*. John Wiley, pp. 413 Hoboken.
- Wynn, R. B. and Stow, D. A. V. (2002). Classification and characterisation of deep-water sediment waves. *Marine Geology* 192, 7-22
- Wynn, R. B., Weaver, P. P. E., Ercilla, G., Stow, D. A. V., and Masson, D. G. (2000a). Sedimentary processes in the Selvag sediment-wave field, NE Atlantic: new insights into the formation of sediment waves by turbidity currents. *Sedimentology* 47, 1181-1197
- Wynn, R. B., Weaver, P. P. E., Ercilla, G., Stow, D. A. V., and Masson, D. G. (2000b). Sedimentary processes in the Selvag sediment-wave field, NE Atlantic: new insights into the formation of sediment waves by turbidity currents. *Sedimentology* 47, 1181-1197.